catalysts

Article

Mutation of Key Residues in β-Glycosidase LXYL-P1-2 for Improved Activity

Jing-Jing Chen, Xiao Liang, Tian-Jiao Chen, Jin-Ling Yang and Ping Zhu *

State Key Laboratory of Bioactive Substance and Function of Natural Medicines, NHC Key Laboratory of Biosynthesis of Natural Products, CAMS Key Laboratory of Enzyme and Biocatalysis of Natural Drugs, Institute of Materia Medica, Chinese Academy of Medical Sciences & Peking Union Medical College, Beijing 100050, China; chenjingjing@imm.ac.cn (J.-J.C.); liangxiao@imm.ac.cn (X.L.); chentianjiao@imm.ac.cn (T.-J.C.); yangjl@imm.ac.cn (J.-L.Y.)

* Correspondence: zhuping@imm.ac.cn; Tel.: +86-10-6316-5197

Abstract: The β-glycosidase LXYL-P1-2 identified from *Lentinula edodes* can be used to hydrolyze 7-β-xylosyl-10-deacetyltaxol (XDT) into 10-deacetyltaxol (DT) for the semi-synthesis of Taxol. Recent success in obtaining the high-resolution X-ray crystal of LXYL-P1-2 and resolving its three-dimensional structure has enabled us to perform molecular docking of LXYL-P1-2 with substrate XDT and investigate the roles of the three noncatalytic amino acid residues located around the active cavity in LXYL-P1-2. Site-directed mutagenesis results demonstrated that Tyr^{268} and Ser^{466} were essential for maintaining the β-glycosidase activity, and the L220G mutation exhibited a positive effect on increasing activity by enlarging the channel that facilitates the entrance of the substrate XDT into the active cavity. Moreover, introducing L220G mutation into the other LXYL-P1-2 mutant further increased the enzyme activity, and the β-D-xylosidase activity of the mutant EP2-L220G was nearly two times higher than that of LXYL-P1-2. Thus, the recombinant yeast GS115-EP2-L220G can be used for efficiently biocatalyzing XDT to DT for the semi-synthesis of Taxol. Our study provides not only the prospective candidate strain for industrial production, but also a theoretical basis for exploring the key amino acid residues in LXYL-P1-2.

Keywords: site-directed mutagenesis; β-glycosidase; enzyme activity; molecular docking; biocatalysis

Citation: Chen, J.-J.; Liang, X.; Chen, T.-J.; Yang, J.-L.; Zhu, P. Mutation of Key Residues in β-Glycosidase LXYL-P1-2 for Improved Activity. *Catalysts* **2021**, *11*, 1042. https://doi.org/10.3390/catal11091042

Academic Editors: Edinson Yara-Varón and Ramon Canela-Garayoa

Received: 7 August 2021
Accepted: 26 August 2021
Published: 28 August 2021

1. Introduction

Enzyme-based biocatalysis has been applied in many areas, especially in pharmaceuticals, chemicals, fragrances, cosmetics, and biofuels [1–5]. The effective catalytic properties of enzymes have promoted their applications. Developments in biotechnology, particularly in the area of protein engineering, have provided important tools for efficiently improving enzyme properties [6–9], such as increasing catalytic efficiency [10] and/or specific substrate recognition [11,12] or improving thermal stability [13–16]. In recent years, more and more protein crystal structures have been resolved with the development of analytic technology. Based on the information obtained by molecular docking and other analysis, the key amino acid residues related to enzyme activity can be speculated, and their roles can be identified through targeted mutation [17,18]. Moreover, the specific amino acid residues of enzyme can be chosen to be precisely designed to improve the enzyme property. This method has the characteristics of simple operation and high success rate, and can obtain mutants with improved properties in a short time [19–21]. Meanwhile, the results obtained through rational design can, in turn, increase the understanding of the enzyme catalytic mechanism, thus further increase the successful rate of beneficial enzyme modification, and also lay a foundation for the functional elucidation of unknown protein [22].

Taxol (generic name: paclitaxel), a well-known blockbuster anticancer drug, has an extremely low content in yew bark [23–26]. However, the content of 7-β-xylosyl-10-deacetyltaxol (XDT), an analogue of Taxol, is much higher than that of Taxol in several

Taxus species, such as *T. wallichiana* and *T. chinese*. The bifunctional β-D-xylosidase/β-D-glucosidase LXYL-P1-2 was identified from *Lentinula edodes*, which belongs to the glycoside hydrolase 3 (GH3) family and shows very low similarity with other known GHs. More importantly, LXYL-P1-2 can remove the C7 xylosyl group from XDT to form 10-deacetyltaxol (DT), which can be acetylated at the C10 position to produce Taxol (Scheme 1) [27,28]. Moreover, LXYL-P1-2 has been successfully expressed in *Pichia pastoris*, and the recombinant yeast can be used as a biocatalyst to convert XDT into DT for the semi-synthesis of Taxol [29–31]. Thus, LXYL-P1-2 has a great potential in the pharmaceutical industry. Recently, the high-resolution X-ray crystal of LXYL-P1-2 has been successfully obtained and its three-dimensional structure has been resolved [32]. On this basis, molecular docking of LXYL-P1-2 and substrate XDT was carried out, and the specific amino acid sites other than catalytic sites were selected, which may play critical roles in enzyme activity. Then, the site-directed mutagenesis of selected noncatalytic residues was conducted to investigate their roles in LXYL-P1-2. Furthermore, the beneficial mutation was introduced into the other LXYL-P1-2 mutant to acquire a mutant with higher activity, which provides the prospective candidate strain for industrial production of Taxol.

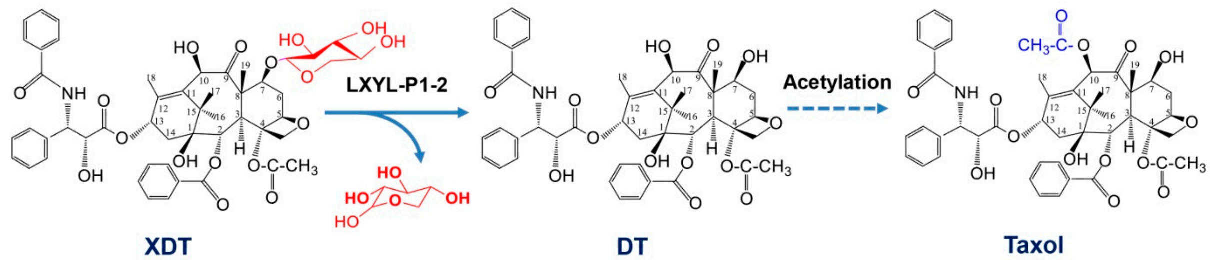

Scheme 1. The β-glycosidase LXYL-P1-2 hydrolyzes the xylosyl group from XDT to produce DT for the semi-synthesis of Taxol. XDT, 7-β-xylosyl-10-deacetyltaxol; DT, 10-deacetyltaxol.

2. Results

2.1. Selection of Mutation Sites

To find the key amino acid residues that affect the activity of the β-glycosidase LXYL-P1-2, molecular docking between the enzyme and the substrate XDT was conducted based on the three-dimensional structure of LXYL-P1-2 (PDB code 6JBS). As shown in Figure 1a, the substrate XDT is in the active cavity of LXYL-P1-2, where the 7-xylosyl group is close to the catalytic sites Asp^{300} and Glu^{529}. In the enzyme-substrate complex model, Glu^{529} provides protons and Asp^{300} performs nucleophilic attack, which is consistent with the catalytic mechanism of other glycosidases. Other than the early confirmed catalytic sites (Asp^{300} and Glu^{529}), three noncatalytic residues Leu^{220}, Tyr^{268}, and Ser^{466}, located around the active cavity of the enzyme, have attracted our attention. We hypothesize that these residues play important roles in enzyme activity of LXYL-P1-2. Among them, Leu^{220} is located at the channel where the substrate enters the active cavity. It is assumed that the XDT may more easily enter the active pocket if Leu^{220} was replaced with Gly^{220} which has a smaller side chain (Figure 1b,c). Moreover, Tyr^{268} is very close to the substrate, and can form hydrogen bonds with the substrate, catalytic sites Asp^{300}, and the surrounding amino acids Trp^{301}. Meanwhile, Ser^{466} is also close to the substrate, and can form the hydrogen bonds with the catalytic sites Glu^{529} and other surrounding amino acids Asp^{109} and Arg^{115} (Figure 1b). The analysis results implied that the existence of these hydrogen bonds may be critical for enzyme activity. Therefore, in order to investigate the roles of these hydrogen bonds, Tyr^{268} and Ser^{466} were mutated into Glu^{268} and Asp^{466}, respectively, in which the numbers of hydrogen bonds formed by Y268E and S466D mutants were decreased (Figure 1d,e).

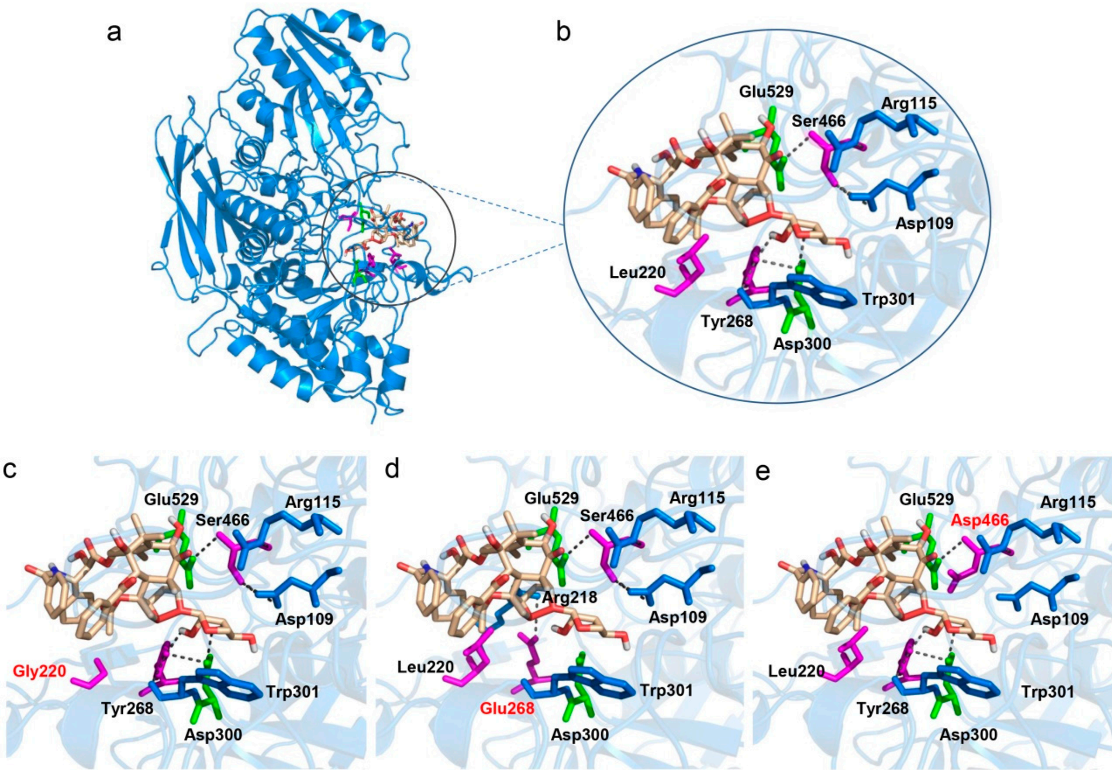

Figure 1. The 3D structure model of the protein–substrate complex. (**a**) Overview of LXYL-P1-2 in complex with XDT. Close-up view of molecular docking of LXYL-P1-2 (**b**) and mutants harboring L220G (**c**), T268E (**d**), and S466D (**e**) mutations with XDT. The carbon atoms of XDT are shown in wheat. The catalytic sites (Asp^{300} and Glu^{529}) are shown in green. The residues (Leu^{220}, Tyr^{268}, and Ser^{466}) predicted to play important roles on enzyme activity are shown in magenta. The mutated sites are shown in red. Hydrogen bonds are shown as dotted lines.

2.2. Measurement of β-Glycosidase Activities of Mutant Strains

In order to investigate the effect of L220G, Y268E, and S466D mutations on the enzyme activity, the corresponding recombinant yeasts were constructed, and their biomass enzyme activities were detected as described previously [33]. As shown in Figure 2a,b, the β-D-xylosidase and β-D-glucosidase activities of GS115-L220G were always higher than those of GS115-P1-2 during the entire fermentation stage. At the induction time of 7 d by methanol, the β-D-xylosidase and β-D-glucosidase activities of GS115-L220G reached 1.27×10^5 U/g and 3.33×10^5 U/g, respectively, which increased by 13% and 25% compared with those of GS115-P1-2 (1.12×10^5 U/g and 2.67×10^5 U/g, respectively). However, the β-D-xylosidase and β-D-glucosidase activities of the mutants GS115-Y268E and GS115-S466D were almost lost. Moreover, the induced recombinant cells were harvested after 7 d of cultivation, and the conversion rates towards XDT by the recombinant cells were also measured. As shown in Figure 2c, the hydrolytic activity on XDT of the mutant GS115-L220G was 1.13 times higher than that of the wild-type. Nevertheless, the hydrolytic activities on XDT of the mutant strains GS115-Y268E and GS115-S466D were significantly decreased or even lost compared with that of the control, indicating that Tyr^{268} and Ser^{466} are essential for maintaining the enzyme activity.

2.3. Effect of L220G Mutation on the Activity of the Other LXYL-P1-2 Mutant EP2

In our previous study, we obtained a highly active mutant EP2 which harbored the T368E mutation in LXYL-P1-2 through directed evolution strategy [34]. To further confirm whether the L220G mutation is beneficial for the further improvement of EP2, we introduced the L220G mutation into EP2, and the enzyme activity of corresponding recombinant yeast was measured. The results showed that the introduction of L220G mutation into the EP2 also led to the improvement of the β-glycosidase activity and the ability to hydrolyze the substrate XDT of the recombinant yeast GS115-EP2-L220G (Figure 3). Moreover, the β-D-xylosidase and the β-D-glucosidase activities of GS115-EP2-L220G were 1.7 times and 1.4 times higher than those of GS115-P1-2, respectively.

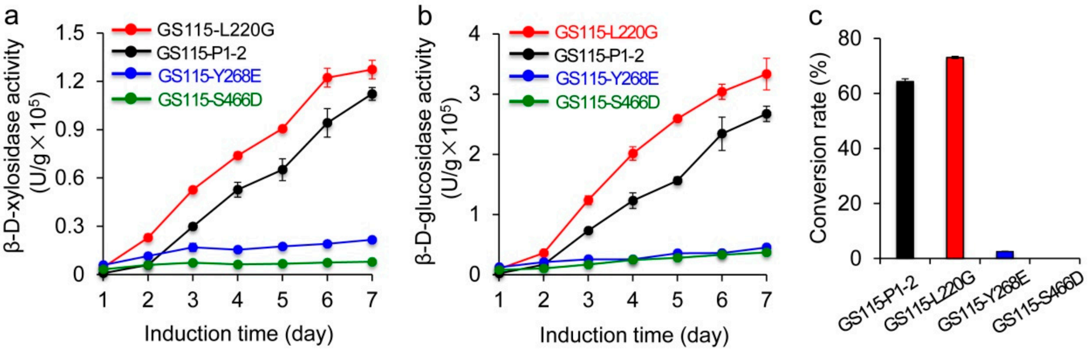

Figure 2. Comparison of β-D-xylosidase activities (**a**) and β-D-glucosidase activities (**b**), as well as conversion rates towards XDT (**c**) among the recombinant yeasts GS115-L220G, GS115-Y268E, and GS115-S466D. The recombinant yeast GS115-P1-2 is used as the control. Data are the mean ± SD. n = 3.

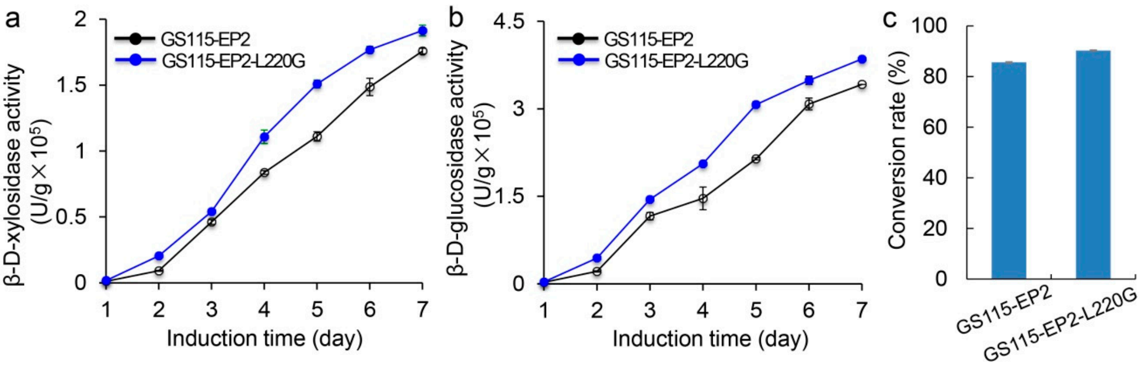

Figure 3. The β-D-xylosidase activities (**a**), β-D-glucosidase activities (**b**), and conversion rates towards XDT (**c**) of the recombinant yeasts GS115-EP2 and GS115-EP2-L220G. Data are the mean ± SD, n = 3.

2.4. Specific β-Glycosidase Activities of the Mutants

To further analyze the specific β-glycosidase activities of the mutants, the recombinant proteins were purified and their activities were evaluated. As shown in Figure 4a, the β-D-xylosidase activities of the mutants P1-2-L220G and EP2-L220G were both increased, which were 1.55 times and 1.17 times of those of the corresponding controls, respectively. Moreover, the mutant EP2-L220G was 1.8 times higher than LXYL-P1-2 in the β-D-xylosidase activity. As EP2-L220G is the mutant harboring the T368E and L220G mutation in LXYL-P1-2, the result indicated that the combination of double mutations exhibited a synergetic effect on increasing the β-D-xylosidase activity. Similarly, the β-D-glucosidase activities of these mutants were also enhanced (Figure 4b), although the increasing degree in β-D-glucosidase activity was less than that in β-D-xylosidase activity.

2.5. Kinetic Analysis of LXYL-P1-2 Mutants against XDT

The kinetic parameters of the mutated enzymes against XDT were determined at the optimal temperature and pH. The results are listed in Table 1. The turnover number (k_{cat}) of P1-2-L220G and EP2-L220G against XDT were significantly increased, which were 3.1-fold and 6.2-fold higher than those of controls, respectively. Meanwhile, the K_m values of the above mutants were also enhanced compared with those of controls. Nevertheless, the catalytic efficiencies (k_{cat}/K_m) of P1-2-L220G and EP2-L220G against XDT were still increased compared with those of LXYL-P1-2 and EP2, respectively. Consequently, the catalytic efficiency of EP2-L220G against XDT was 1.7-fold higher than that of LXYL-P1-2.

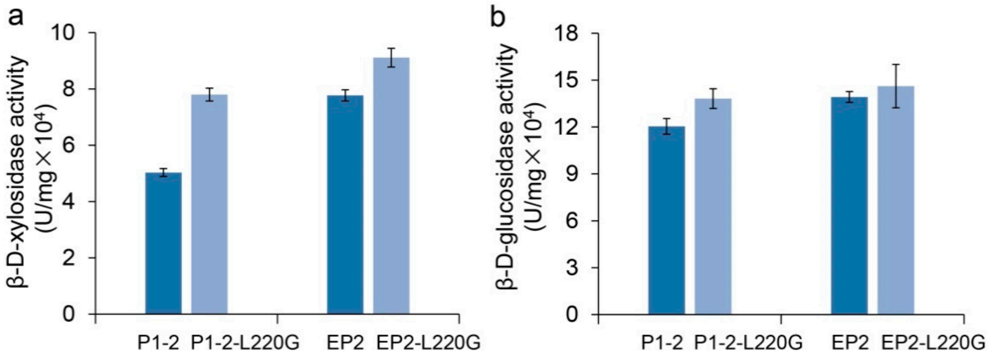

Figure 4. Specific activities of different L220G mutants against PNP-Xyl (**a**) and PNP-Glc (**b**). P1-2-L220G and EP2-L220G are the enzymes harboring L220G mutation. LXYL-P1-2 and P1-2-EP2 are used as controls, respectively. Data are the mean ± SD, n = 3.

Table 1. Kinetic parameters for the hydrolysis of XDT by mutants harboring L220G mutation.

	V_{max} (μmol L^{-1} min^{-1})	K_m (mmol L^{-1})	k_{cat} (s^{-1})	k_{cat}/K_m (mmol L^{-1} s^{-1})
LXYL-P1-2	7.28 (±0.13)	0.50 (±0.01)	4.37 (±0.08)	8.72 (±0.09)
P1-2-L220G	22.42 (±2.42)	1.47 (±0.15)	13.44 (±1.45)	9.17 (±0.22) *
EP2	3.30 (±0.04)	0.15 (±0.01)	1.98 (±0.03)	13.44 (±0.76) ***
EP2-L220G	20.70 (±0.60)	0.86 (±0.10)	12.41 (±1.01)	14.45 (±0.60) ***

Note: Data are the mean (± SD), n = 3. * $p < 0.05$ vs. LXYL-P1-2 and *** $p < 0.001$ vs. LXYL-P1-2.

3. Discussion

Based on the available structure information of LXYL-P1-2, the molecular docking between the LXYL-P1-2 and XDT was conducted. The three noncatalytic amino acid residues Leu^{220}, Tyr^{268}, and Ser^{466}, located around the active cavity, were speculated to have greater impacts on the activity of the enzyme. Thus, these three sites were chosen for mutation. Through the site-directed mutagenesis of LXYL-P1-2, we obtained three variants including P1-2-L220G, P1-2-Y268E, and P1-2-S466D. The β-D-xylosidase and β-D-glucosidase activities of P1-2-Y268E and P1-2-S466D were almost completely lost, indicating that Tyr^{268} and Ser^{466} are very important for maintaining the spatial structure and physical and chemical environment of the active center. As Tyr^{268} and Ser^{466} form the hydrogen bonds with the glycoside structure of XDT, the catalytic sites and the surrounding amino acids, the Y268E or the S466D mutation may decrease the stability of the substrate in the active pocket of enzyme, and change the protein conformation near the catalytic sites, which is not conducive to the progress of the catalytic reaction. Moreover, as we expected, the β-D-xylosidase and β-D-glucosidase activities of P1-2-L220G and its ability to hydrolyze the substrate XDT were much higher than those of the control, which suggest that the L220G mutation has exhibited the positive effect on increasing the enzyme activity. Similar phenomenon was also observed when the L220G mutation was introduced into EP2, resulting in mutant EP2-L220G with higher β-D-xylosidase activity than that of the control. Furthermore, it was found that the maximum reaction rate (V_{max}) and turnover number (k_{cat}) of the mutants for hydrolyzing XDT were significantly higher than those of the controls, demonstrating that the L220G mutation is an important factor for increasing the conversion rate of XDT in the biocatalytic reaction. In addition, we observed that the effect of the L220G mutation on the improvement of β-D-glucosidase activity is not obvious, possibly as the complex model was based on the substrate XDT, and the mutation was not necessarily suitable for the enhancement of β-D-glucosidase activity. Thus, the roles of amino acid residues involved in the hydrolysis of β-xyloside may not be exactly the same as those in hydrolysis of β-glucoside.

To further explore how the L220G and T368E mutations in EP2-L220G affect the enzyme activity, molecular docking between the mutant EP2-L220G and the substrate XDT was conducted. As shown in Figure 5, Leu^{220} is located at the channel through which the substrate enters the active cavity. Turning Leu into Gly with a smaller side chain volume may allow the substrate to enter the active cavity more smoothly. Meanwhile, T368E mutation may alter the profile of the loop near the active pocket, which may be more conducive to the catalytic reaction.

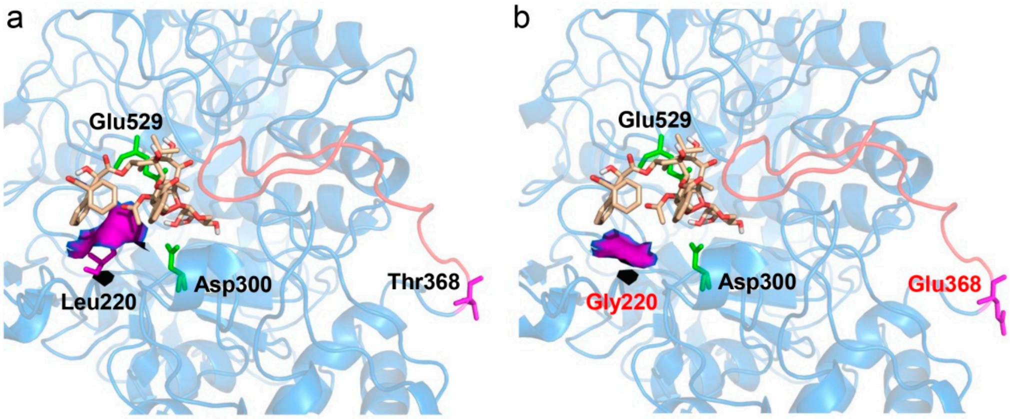

Figure 5. Partial view of molecular docking of LXYL-P1-2 (**a**) and EP2-L220G (**b**) with XDT. The carbon atoms of XDT are shown in wheat. The catalytic sites (Asp^{300} and Glu^{529}) are shown in green. The amino acids in the position 220 and 368 are shown in magenta. The alteration of the loop near the active pocket by T368E mutation is shown in red.

4. Materials and Methods

4.1. Plasmids and Strains

The recombinant expression plasmids pPIC3.5K-LXYL-P1-2 and pPIC3.5K-LXYL-P1-2-EP2 harboring the *lxyl-p1-2* and *lxyl-p1-2-EP2*, respectively were previously constructed in our laboratory. The *Pichia pastoris* GS115-P1-2 and GS115-EP2 were constructed by transforming the corresponding plasmid into the host strain *P. pastoris* GS115 (Mut^+). All the strains were preserved at −80 °C prior to use.

4.2. Molecular Docking between LXYL-P1-2 the Substrate XDT

Molecular docking between LXYL-P1-2 (PDB code 6JBS) and XDT substrate was conducted using AutoDockTools software. The center point of the Grid Box was set in the middle of the active cavity, and the range of the Grid Box was set as 26 × 26 × 26, which ensures the Grid Box covers the whole active cavity.

4.3. Mutation of Key Residues in LXYL-P1-2

Site-directed mutations in LXYL-P1-2 were conducted through whole-plasmid amplification. Primers used are listed in Table 2. First, the expression plasmid pPIC3.5K-LXYL-P1-2 was used as a template in the PCR reactions. PCR was performed with Phusion DNA polymerase using the following pairs of primers: p1-2-L220G-F/ p1-2-L220G-R, p1-2-Y268E-F/p1-2-Y268E-R, and p1-2-S466D-F/p1-2-S466D-R, respectively. The PCR run started with a first cycle of 30 s at 98 °C, and followed by 30 cycles of 10 s at 98 °C, 30 s at 60 °C, and 1 min at 72 °C. The PCR was ended with an extension step of 10 min at 72 °C. Then, the PCR products were purified and digested by Dpn I at 37 °C for 3 h and transformed into DMT competent cells (Transgen, Beijing, China). The corresponding plasmids were extracted. Finally, after verification by DNA sequencing, the recombinant plasmids were transformed into *P. pastoris* GS115 and the transformants were screened as mentioned previously [33]. The resulting mutant strains were referred to as GS115-L220G, GS115-Y268E, and GS115-S466D, respectively. For the construction of the variant harboring L220G mutation in EP2, the PCR amplification was conducted using the plasmid pPIC3.5K-LXYL-P1-2-EP2 as a template and the primers p1-2-L220G-F/p1-2-L220G-R. The corresponding strain was constructed as mentioned above and referred to as GS115-EP2-L220G.

Table 2. Primers used for construction of *lxyl-p1-2* variants.

Primer	Sequence (5′ → 3′)
p1-2-L220G-F	AGAAAT GGA TATATCGACATCGACGGAGTT
p1-2-L220G-R	GATGTCGATATA TCC ATTTCTCGATGTTTC
p1-2-Y268E-F	CATGTGTTCC GAA AACCGTATCAACAACAC
p1-2-Y268E-R	TACGGTT TTC GGAACACATGATATGATTCG
p1-2-S466D-F	GGCGGA GAC GGGTCGGCACTTTCACCATAC
p1-2-S466D-R	GTGCCGACCC GTC TCCGCCTCCTGTTGTC

Note: Mutated bases are boxed.

4.4. Measurement of β-Glycosidase Activities of Mutant Strains

The mutant strains constructed above were firstly grown at 30 °C and 200 rpm for 60 h in 100 mL buffered minimal glycerol complex medium (BMGY) medium (20 g/L tryptone, 13.4 g/L YNB, 10 g/L yeast extract, 10 g/L glycerol, 0.4 mg/L biotin, 100 mmol/L potassium phosphate buffer, pH 6.0). In order to induce the heterologous protein expression, 1 mL methanol was added in the 100 mL culture every day. Meanwhile, the β-D-xylosidase and β-D-glucosidase activities were analyzed by periodic sampling. Briefly, the cells were firstly collected via centrifugation and washed twice with dH_2O. After resuspending the cells in dH_2O in the same volume of culture broth, 10 µL cell suspension was mixed with 100 µL p-nitrophenyl-β-D-xylopyranoside (PNP-Xyl, 5 mmol/L) or p-nitrophenyl-β-D-glucopyranoside (PNP-Glc, 5 mmol/L), and the β-glycosidase activities were measured as described previously [34]. Furthermore, the conversion rates towards XDT by the mutant strains were also measured. After inducing protein expression for 7 days, the recombinant cells were collected and freeze dried. The dried cells (16 mg) were resuspended in 1.8 mL of 0.1 M sodium acetate buffer (pH 4.0), to which 200 µL of 100 mg/mL XDT was added. The reaction was performed at 45 °C for 24 h. Finally, the reaction was stopped by adding menthol. The products were assayed via HPLC and conversion rate was calculated as described previously [34].

4.5. Purification of Recombinant LXYL-P1-2 Mutants

After 7 days of induction, the recombinant yeasts harboring L220G mutation were collected, and the proteins were purified as described in our previous report [33]. Briefly, the cells were harvested by centrifugation at 10,000× *g* for 10 min, then washed and resuspended in buffer A (20 mM Tris-HCl, pH 8.0). The cells were lysed by high-pressure cell disruption (APV-2000, SPX Corporation, Charlotte, NC, USA) for 10 cycles, and the cellular debris was removed by centrifugation at 16,000× *g* for 30 min. After filtration through a 0.45 µm filter, the supernatant was subjected to a 2 mL nickel bonded affinity chromatography, and sequentially eluted by 20 mM, 60 mM, and 200 mM imidazole solution (pH 8.0). The elution fraction from 60 mM imidazole was merged together and concentrated. Then, the concentrated sample was further purified through preparative high performance liquid chromatography by using Agilent Zorbax Bio Series GF-450 column. Next, 500 µL supernatant was subjected to the column and eluted by 0.1 M potassium phosphate buffer (pH 8.0) at the flow rate of 0.5 mL/min and the UV wavelength of 280 nm. Finally, the purified fractions were concentrated by ultrafiltration, and flash frozen at −80 °C.

4.6. Enzyme Activities and Kinetics Parameters Measurement of LXYL-P1-2 Mutants

The β-D-xylosidase and β-D-glucosidase activities of the purified proteins harboring L220G mutation were measured using substrate PNP-Xyl or PNP-Glc, as mentioned in our previous report [34]. Concretely, 50 µL of 5 mmol/L PNP-Xyl or PNP-Glc was added into 10 µL of 0.1 mg/mL enzyme in 50 mmol/L sodium acetate buffer with pH 5.0, and the reaction was performed under 50 °C for 20 min. Reactions were stopped by adding 1 mL saturated $Na_2B_4O_7$ solution. The enzymatic activity was assayed using spectrophotometry based on the absorbance at 405 nm. One unit of activity was defined as the amount of enzyme that catalyzed the formation of 1 nmol/L p-nitrophenol per minute. The kinetic parameters against XDT of the mutants harboring L220G mutation were evaluated as described previously [34].

5. Conclusions

In conclusion, we investigated the roles of the three noncatalytic amino acid residues located around the active cavity in LXYL-P1-2. The site-directed mutagenesis demonstrated that Tyr^{268} and Ser^{466} were essential for maintaining the β-glycosidase activity of LXYL-P1-2 and the L220G mutation exhibited the positive effect on increasing activity by enlarging the channel that facilitates the entrance of the substrate XDT into the active cavity. Moreover, introducing L220G mutation into the highly active mutant EP2 further increased the enzyme activity, and the β-D-xylosidase activity of the mutant EP2-L220G was nearly two times higher than that of LXYL-P1-2. Thus, the recombinant yeast GS115-EP2-L220G can be used for efficiently biocatalyzing XDT to DT for the semi-synthesis of Taxol. Our study provides not only the prospective candidate strain for industrial production, but also a theoretical basis for exploring the key amino acid residues in LXYL-P1-2.

Author Contributions: Conceptualization, J.-J.C. and X.L.; methodology, J.-J.C., X.L. and T.-J.C.; validation, J.-J.C. and X.L.; formal analysis, J.-J.C., X.L. and T.-J.C.; writing—original draft preparation, J.-J.C.; writing—review and editing, J.-J.C., J.-L.Y. and P.Z.; and funding acquisition, P.Z. All authors have read and agreed to the published version of the manuscript.

Funding: This research was funded by the National Key Research and Development Program of China (Grant Nos. 2018YFA0901900 and 2020YFA0908003), National Natural Science Foundation of China (Grant No. 81573325), PUMC Disciplinary Development of Synthetic Biology (Grant No. 201920100801).

Data Availability Statement: Data are contained within the article.

Conflicts of Interest: The authors declare no conflict of interest.

References

1. Chapman, J.; Ismail, A.E.; Dinu, C.Z. Industrial applications of enzymes: Recent advances, techniques, and outlooks. *Catalysts* **2018**, *8*, 238. [CrossRef]
2. Choi, J.-M.; Han, S.-S.; Kim, H.-S. Industrial applications of enzyme biocatalysis: Current status and future aspects. *Biotechnol. Adv.* **2015**, *33*, 1443–1454. [CrossRef]
3. Kirk, O.; Borchert, T.V.; Fuglsang, C.C. Industrial enzyme applications. *Curr. Opin. Biotechnol.* **2002**, *13*, 345–351. [CrossRef]
4. Chu, J.; Yue, J.; Qin, S.; Li, Y.; Wu, B.; He, B. Biocatalysis for rare ginsenoside Rh2 production in high level with co-immobilized UDP-glycosyltransferase Bs-YjiC mutant and sucrose synthase AtSuSy. *Catalysts* **2021**, *11*, 132. [CrossRef]
5. Millán, A.; Sala, N.; Torres, M.; Canela-Garayoa, R. Biocatalytic transformation of 5-hydroxymethylfurfural into 2, 5-di (hydroxymethyl) furan by a newly isolated *Fusarium striatum* strain. *Catalysts* **2021**, *11*, 216. [CrossRef]
6. Bornscheuer, U.T.; Pohl, M. Improved biocatalysts by directed evolution and rational protein design. *Curr. Opin. Chem. Biol.* **2001**, *5*, 137–143. [CrossRef]
7. Böttcher, D.; Bornscheuer, U.T. Protein engineering of microbial enzymes. *Curr. Opin. Microbiol.* **2010**, *13*, 274–282. [CrossRef] [PubMed]
8. Kazlauskas, R.J.; Bornscheuer, U.T. Finding better protein engineering strategies. *Nat. Chem. Biol.* **2009**, *5*, 526–529. [CrossRef]
9. Rubingh, D.N. Protein engineering from a bioindustrial point of view. *Curr. Opin. Biotechnol.* **1997**, *8*, 417–422. [CrossRef]
10. Li, Y.; Song, K.; Zhang, J.; Lu, S. A computational method to predict effects of residue mutations on the catalytic efficiency of hydrolases. *Catalysts* **2021**, *11*, 286. [CrossRef]
11. Svensson, B. Protein engineering in the α-amylase family: Catalytic mechanism, substrate specificity, and stability. *Plant Mol. Biol.* **1994**, *25*, 141–157. [CrossRef]
12. Perugino, G.; Strazzulli, A.; Mazzone, M.; Rossi, M.; Moracci, M. Effects of random mutagenesis and in vivo selection on the specificity and stability of a thermozyme. *Catalysts* **2019**, *9*, 440. [CrossRef]

13. Yang, H.; Liu, L.; Li, J.; Chen, J.; Du, G. Rational design to improve protein thermostability: Recent advances and prospects. *ChemBioEng Rev.* **2015**, *2*, 87–94. [CrossRef]
14. Zamost, B.L.; Nielsen, H.K.; Starnes, R.L. Thermostable enzymes for industrial applications. *J. Ind. Microbiol. Biot.* **1991**, *8*, 71–81. [CrossRef]
15. Lehmann, M.; Wyss, M. Engineering proteins for thermostability: The use of sequence alignments versus rational design and directed evolution. *Curr. Opin. Biotechnol.* **2001**, *12*, 371–375. [CrossRef]
16. Ayadi, D.Z.; Sayari, A.H.; Hlima, H.B.; Mabrouk, S.B.; Mezghani, M.; Bejar, S. Improvement of *Trichoderma reesei* xylanase II thermal stability by serine to threonine surface mutations. *Int. J. Biol. Macromol.* **2015**, *72*, 163–170. [CrossRef]
17. Bao, X.; Huang, X.; Lu, X.; Li, J.-J. Improvement of hydrogen peroxide stability of *Pleurotus eryngii* versatile ligninolytic peroxidase by rational protein engineering. *Enzyme Microb. Technol.* **2014**, *54*, 51–58. [CrossRef] [PubMed]
18. Jaafar, N.R.; Ayob, S.N.; Abd Rahman, N.H.; Bakar, F.D.A.; Murad, A.M.A.; Illias, R.M. Rational protein engineering of α-L-arabinofuranosidase from *Aspergillus niger* for improved catalytic hydrolysis efficiency on kenaf hemicellulose. *Process Biochem.* **2021**, *102*, 349–359. [CrossRef]
19. Cheng, Y.-S.; Chen, C.-C.; Huang, J.-W.; Ko, T.-P.; Huang, Z.; Guo, R.-T. Improving the catalytic performance of a GH11 xylanase by rational protein engineering. *Appl. Microbiol. Biotechnol.* **2015**, *99*, 9503–9510. [CrossRef]
20. Han, C.; Li, W.; Hua, C.; Sun, F.; Bi, P.; Wang, Q. Enhancement of catalytic activity and thermostability of a thermostable cellobiohydrolase from *Chaetomium thermophilum* by site-directed mutagenesis. *Int. J. Biol. Macromol.* **2018**, *116*, 691–697. [CrossRef]
21. Oh, E.-J.; Lee, Y.-J.; Chol, J.; Seo, M.S.; Lee, M.S.; Kim, G.A.; Kwon, S.-T. Mutational analysis of *Thermus caldophilus* GK24 beta-glycosidase: Role of His119 in substrate binding and enzyme activity. *J. Microbiol. Biotech.* **2008**, *18*, 287–294.
22. Lutz, S. Beyond directed evolution—Semi-rational protein engineering and design. *Curr. Opin. Biotechnol.* **2010**, *21*, 734–743. [CrossRef] [PubMed]
23. Cragg, G.M. Paclitaxel (Taxol): A success story with valuable lessons for natural product drug discovery and development. *Med. Res. Rev.* **1998**, *18*, 315–331. [CrossRef]
24. Liu, W.C.; Gong, T.; Zhu, P. Advances in exploring alternative Taxol sources. *RSC Adv.* **2016**, *6*, 48800–48809. [CrossRef]
25. McGuire, W.P.; Rowinsky, E.K.; Rosenshein, N.B.; Grumbine, F.C.; Ettinger, D.S.; Armstrong, D.K.; Donehower, R.C. Taxol: A unique antineoplastic agent with significant activity in advanced ovarian epithelial neoplasms. *Ann. Intern. Med.* **1989**, *111*, 273–279. [CrossRef] [PubMed]
26. Stierle, A.; Strobel, G.; Stierle, D. Taxol and taxane production by *Taxomyces andreanae*, an endophytic fungus of Pacific yew. *Science* **1993**, *260*, 214–216. [CrossRef] [PubMed]
27. Cheng, H.L.; Zhao, R.Y.; Chen, T.J.; Yu, W.B.; Wang, F.; Cheng, K.D.; Zhu, P. Cloning and characterization of the glycoside hydrolases that remove xylosyl groups from 7-β-xylosyl-10-deacetyltaxol and its analogues. *Mol. Cell Proteomics* **2013**, *12*, 2236–2248. [CrossRef] [PubMed]
28. Li, B.J.; Wang, H.; Gong, T.; Chen, J.J.; Chen, T.J.; Yang, J.L.; Zhu, P. Improving 10-deacetylbaccatin III-10-β-*O*-acetyltransferase catalytic fitness for Taxol production. *Nat. Commun.* **2017**, *8*, 15544. [CrossRef]
29. Liu, W.C.; Gong, T.; Wang, Q.H.; Liang, X.; Chen, J.J.; Zhu, P. Scaling-up Fermentation of *Pichia pastoris* to demonstration-scale using new methanol-feeding strategy and increased air pressure instead of pure oxygen supplement. *Sci. Rep.* **2016**, *6*, 18439. [CrossRef]
30. Liu, W.C.; Zhu, P. Pilot studies on scale-up biocatalysis of 7-β-xylosyl-10-deacetyltaxol and its analogues by an engineered yeast. *J. Ind. Microbiol. Biot.* **2015**, *42*, 867–876. [CrossRef]
31. Yu, W.B.; Liang, X.; Zhu, P. High-cell-density fermentation and pilot-scale biocatalytic studies of an engineered yeast expressing the heterologous glycoside hydrolase of 7-β-xylosyltaxanes. *J. Ind. Microbiol. Biot.* **2013**, *40*, 133–140. [CrossRef] [PubMed]
32. Yang, L.; Chen, T.-J.; Wang, F.; Li, L.; Yu, W.-B.; Si, Y.-K.; Chen, J.-J.; Liu, W.-C.; Zhu, P.; Gong, W. Structures of β-glycosidase LXYL-P1-2 reveals the product binding state of GH3 family and a specific pocket for Taxol recognition. *Commun. Biol.* **2020**, *3*, 1–8. [CrossRef] [PubMed]
33. Chen, J.-J.; Liang, X.; Wang, F.; Wen, Y.-H.; Chen, T.-J.; Liu, W.-C.; Gong, T.; Yang, J.-L.; Zhu, P. Combinatorial mutation on the β-glycosidase specific to 7-β-xylosyltaxanes and increasing the mutated enzyme production by engineering the recombinant yeast. *Acta Pharm. Sin. B* **2019**, *9*, 626–638. [CrossRef] [PubMed]
34. Chen, J.J.; Liang, X.; Li, H.X.; Chen, T.J.; Zhu, P. Improving the catalytic property of the glycoside hydrolase LXYL-P1–2 by directed evolution. *Molecules* **2017**, *22*, 2133. [CrossRef]